Geochimica et Cosmochimica Acta 420 (2026) 148–160

Contents lists available at ScienceDirect

Geochimica et Cosmochimica Acta

journal homepage: www.elsevier.com/locate/gca

Lability of riverine particulate organic carbon increased by water storage and extreme drought-heatwave events

Jixuan Lyu [a,b], Caroline L. Peacock [b], Yifan Zhang [a], Tao Liu [c], Yong Shi [a], Xiaomei Xu [a], Shengjing Liu [a], Yubing Qu [a], Shuo Zhang [c], Guang Yang [a], Dong Peng [a,d], Chonghao Chen [a], Xin Zhou [e], Yanxu Zhang [d], Jianhua Gao [a,c,*]

[a] School of Geography and Ocean Science, Ministry of Education Key Laboratory for Coast and Island Development, Nanjing University, Nanjing, Jiangsu Province, China
[b] University of Leeds, School of Earth and Environment, Leeds LS2 9JT, UK
[c] Collaborative Innovation Center of South China Sea Studies, Nanjing University, Nanjing, Jiangsu Province, China
[d] School of Atmospheric Sciences, Nanjing University, Nanjing, Jiangsu Province, China
[e] Plateau Atmosphere and Environment Key Laboratory of Sichuan Province, School of Atmospheric Sciences, Chengdu University of Information Technology, Chengdu, China

A R T I C L E I N F O

Associate editor: Edward Hornibrook

Keywords:
Lability
Particulate organic carbon
Reservoir
Extreme weather events

A B S T R A C T

Rivers are increasingly affected by dams and reservoirs, which impact the source and transport of riverine particulate organic carbon (POC), and by extreme events, which present an important climatic stressor for river ecosystems. How and to what extent water regulation and extreme events affect POC lability, however, remain poorly constrained. By studying the POC characteristics within the Yangtze River Basin in normal and extreme drought-heatwave years, we find that during a normal year water storage by the Three Gorges Reservoir increases the proportion of algae-derived POC (by 26 ± 4%) compared to water drainage, leading to a higher proportion of labile POC and younger POC age. During the extreme drought-heatwave year, the drought-heatwave event increases proportions of algae-derived POC and labile POC (by 19 ± 11% and 18 ± 8%, respectively) in the whole Yangtze River Basin, with a greater increase in the Three Gorges Reservoir (by 34 ± 7% and 29 ± 3%, respectively; compared with the non-Three Gorges Reservoir areas, $P < 0.01$), whilst resulting in a 29 ± 6% reduction in export POC flux to the East China Sea. We use our findings from the Yangtze River Basin to assess the global impact of dams and reservoirs, and estimate that the global riverine export POC flux has decreased from pre-dam 190 ± 5 Tg C/yr to post-dam 97 ± 48 Tg C/yr. We also posit that the additional increase in POC lability and decrease in export POC flux during an extreme drought-heatwave event in the Yangtze River Basin occurs in other major river systems as well. Combined we assert that more frequent extreme drought-heatwave events will compound the effects of damming, resulting in an increasingly labile and thus more readily remineralized riverine POC source and a decreasing export POC flux into the near-shore environment. Our results provide critical insights into assessing and mitigating the effects of combined damming and extreme drought-heatwave events on the organic carbon cycle in river systems.

1. Introduction

Rivers are an important link between the terrestrial and marine carbon pools (Galy et al., 2008; Regnier et al., 2022). They can transport a large amount of terrestrial particulate organic carbon (POC) to marginal seas (200 Tg C/yr), playing a vital role in regulating the global carbon cycle (Blair and Aller, 2012; Galy et al., 2015). The transfer of terrestrial POC to the marine environment, however, is being increasingly disturbed by human activities and climate change (Best, 2019).

The impact of human activities in the form of dams and their associated reservoirs on rivers is becoming increasingly prominent (Grill et al., 2019; Syvitski et al., 2005; Tessler et al., 2015). Dams can directly trap a large amount of the terrestrial POC and increase the potential role of phytoplankton biomass in riverine biogeochemistry (Lyu et al., 2023;

* Corresponding author at: School of Geography and Ocean Science, Ministry of Education Key Laboratory for Coast and Island Development, Nanjing University, Nanjing, Jiangsu Province, China.
E-mail address: jhgao@nju.edu.cn (J. Gao).

https://doi.org/10.1016/j.gca.2026.03.056
Received 21 May 2025; Accepted 29 March 2026
Available online 4 April 2026
0016-7037/

Maavara et al., 2017). In particular, intra-annual water regulation by dams is the major factor affecting trapping efficiency and could alter the hydrological and ecological processes of rivers in a short time (Derrien et al., 2019; Grill et al., 2015; Lu et al., 2023), which might, in turn, change the sources of POC (e.g., the autochthonous source). The consequences of damming to POC are critically important because different sources of POC have different compositional characteristics and lability, not only may lead to new conditions in the short term but can also influence the long-term terrestrial net C and N storage and feedback to the atmosphere, which help control their remineralization and storage in both short and long term, as well as their feedback to atmosphere (Belay-Tedla et al., 2009; Galy et al., 2015; Repasch et al., 2021; Schädel et al., 2014).

In addition to human activities, rivers are also being severely affected by anthropogenic climate change, which has increased the frequency and intensity of extreme events (e.g., heatwaves, drought, storms, and floods) across the world (Coronese et al., 2019; Perkins-Kirkpatrick and Lewis, 2020; Russo et al., 2014). Against the background of climate change, heatwaves occur more frequently, providing a favorable environment for the rapid intensification of drought (Teuling, 2018; Wang et al., 2016). Higher temperatures may potentially increase algae biomass and enlarge the area and duration of algal blooms (Tian et al., 2013), which may severely impact the river ecosystem and change POC composition and lability, while precipitation could substantially affect POC flux (Ludwig et al., 1996). These changes in the lability and flux of riverine POC may have important consequences for carbon storage in estuaries and coasts, adding to the effect of water regulation on the global carbon cycle and budgets, yet these changes are poorly constrained.

The Yangtze River, which is recognized as one of the largest sediment-exporting rivers globally and has been ranked fourth in annual sediment load during its high-sediment-yield period, delivers substantial POC to the East China Sea (Li et al., 2016; Liu et al., 2019; Yao et al., 2015). To fill the critical knowledge gap, we chose the Yangtze River as a specific case due to its recent exposure to an extreme weather event and evident anthropogenic alterations. In the summer of 2022, the northern hemisphere experienced an extreme heatwave event, with extremely high temperatures and severe drought in many countries (Kennedy, 2022; Toreti et al., 2022); notably, a record-breaking drought-heatwave event occurred in the Yangtze River Basin (Mallapaty, 2022), with the water level and sediment loads in the middle-lower reaches at their lowest since historical records began (MWRC, 1990–2022). Additionally, the construction of the Three Gorges Dam and cascade dams upstream since 2003, however, has had a significant impact on the terrestrial POC flux, decreasing this from ~8.0 Tg C/yr pre-dams to ~1.5 Tg C/yr post-dams (Li et al., 2015). Moreover, as the sink of organic carbon (OC) from the Yangtze River, the East China Sea has also been affected, where the sedimentary deposition flux of total OC (i.e., the rate at which OC is buried in seabed sediments) in the East China Sea decreased by 48% after dam construction (Wang et al., 2020). Despite the substantial changes in POC flux, the extent to which dams affect the riverine carbon sources and lability, the knock-on implications for carbon budgets, and the further impact of extreme events on the carbon cycle under the context of global climate change, are still unclear.

In this study, we investigate the impact of dams and an extreme drought-heatwave event on POC characteristics within the Yangtze River Basin. The main objectives of this work are to: (a) quantitatively determine how POC sources and lability in the Yangtze River Basin vary due to water regulation by dams, (b) analyze the extent to which POC flux and lability in the Yangtze River Basin are affected by the combined impact of dams and an extreme drought-heatwave event, and (c) provide an outlook for other large and rapidly changing river basins.

2. Material and methods

2.1. Regional settings

The Yangtze River is 6300 km long and covers a basin area of around 1.8×10^6 km^2 (Fig. 1). It is geographically divided into upper, middle, and lower reaches. The upper reaches, extending from the Qinghai-Tibetan Plateau to Yichang City, are characterized by mountainous topography with high relief at elevations over 3000 m and are mainly distributed with Paleozoic carbonate rocks, Mesozoic sedimentary and igneous rocks. The segment upstream of Yibin City is called the Jinsha River, and the major tributaries of the upper reaches include Yalong, Min, Jialing, and Wu Rivers. The middle-lower reaches mainly consist of riverine plains, and are overlain by the Paleozoic marine, Mesozoic sedimentary rocks, and Quaternary loose sediments of fluvial and lacustrine facies, where two large lake systems (the Dongting and Poyang lakes) and the Han River interact closely with the mainstem. Controlled by the Asian monsoon, the annual precipitation in the basin generally ranges from <500 mm/yr in the source region to >1600 mm/yr in the middle-lower reaches. The annual and monthly water discharge and sediment load of the Yangtze River are shown in Figs. S1 and S2.

So far, there are 12 giant reservoirs in the upper mainstem of the Yangtze River (Fig. 1b), among which the Three Gorges Reservoir (TGR) is currently the largest hydropower project in the world (impounded in 2003), and the other 11 reservoirs upstream began impoundment in succession since 2010. More detailed information about the dam-associated reservoirs is provided in Table S1. In terms of water regulation within a year, the TGR is the most typical for its overall three periods (Fig. 2a). Drainage period (January–June): to supply water for the lower reaches and prepare for the wet season, the water level of the TGR must be lowered to 145 m. Flood control period (June–September): in this stage, the TGR operates at the flood control limit level of 145 m. Storage period (September–December): with the end of the wet season, the TGR begins to store more incoming water and gradually raises the water level to 175 m to ensure shipping, water replenishment, and power generation.

2.2. Sampling

We collected suspended particulate matter (SPM) within the Yangtze River Basin in July 2021, October 2021, and August 2022 (Fig. 1c). In July 2021, the mainstem comprised 14 sampling stations, and the tributaries comprised 5 sampling stations. In October 2021, the mainstem comprised 15 sampling stations, and no samples were collected in the tributaries. In August 2022, the mainstem comprised 15 sampling stations, and the tributaries comprised 3 sampling stations. The extreme drought-heatwave event in August 2022 caused the water level of the Yangtze River Basin to drop considerably (Fig. S3). We collected samples from the upper reaches at GYY to the estuary at XLJ, including sampling stations GYY, JS, XJB, and PZH within cascade reservoir impacted areas in the upper reaches and WS, ZG, and YC, which make up the TGR in the mid reaches (Fig. 1c).

Sampling was conducted during three distinct hydrological conditions (Fig. 2) – water drainage in a normal hydrological year, during which the reservoir operates primarily in flood-control mode (represented by July 2021), water storage in a normal hydrological year (represented by October 2021), and then extreme drought-heatwave event (represented by August 2022) marked by severe hydrological and meteorological anomalies despite being in the water drainage period within the wet season. July, August, and October are all in the wet season of the year (from May to October). During the wet season, the Yangtze River supplies over 86% of the annual sediment load to the East China Sea (MWRC, 1990–2022), suggesting our samples are representative of the majority of POC exported by the Yangtze River.

Sub-surface water samples (0.5 m underwater, 150 L total) were collected from a cross-section in the main channel using acid-washed 25-

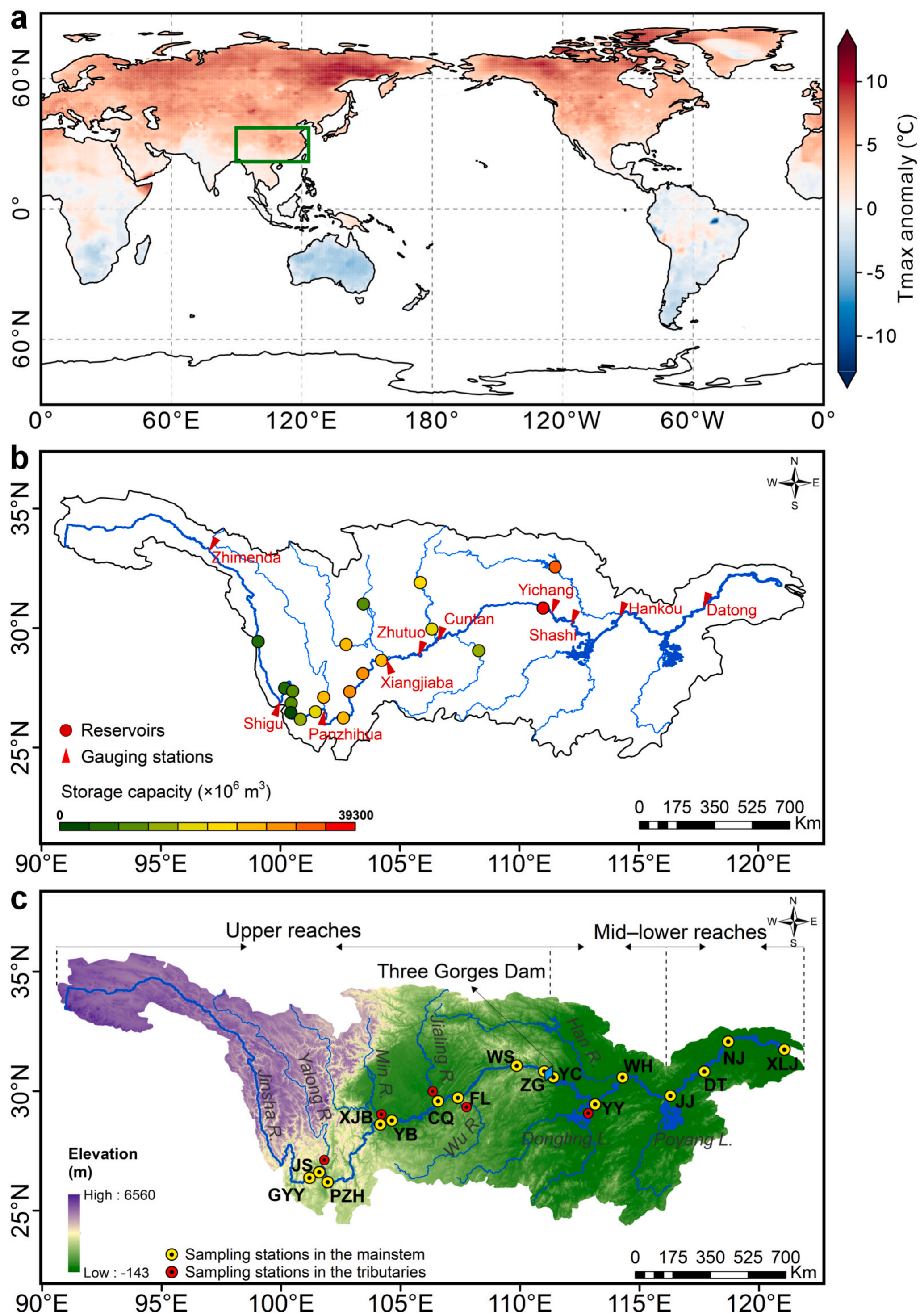

Fig. 1. Study area showing sampling stations. (a) Average surface air temperature anomaly (°C) for June–September 2022 worldwide, relative to the average for the 1991–2020 reference period. The data are from the CPC Global Unified Temperature data provided by the NOAA PSL (). The green square shows the location of the Yangtze River Basin. (b) Locations of giant dam-associated reservoirs and gauging stations in the mainstem of the Yangtze River. (c) Sampling stations in the Yangtze River Basin in the mainstem and tributaries. GYY at the Guanyinyan Reservoir was only sampled in October 2021, and XJB at the Xiangjiaba Reservoir was only sampled in August 2022.
available at: https://psl.noaa.gov

L polyethylene samplers, and sediment was subsequently recovered by filtering the water under vacuum through pre-combusted (450 °C for 3 h) glass fiber filters (nominal pore size: 0.7 μm, Whatman GF/F). All the filtered samples were freeze-dried and stored at −20 °C for further analysis.

2.3. Measurement of POC, particulate nitrogen (PN), and labile POC (LPOC) contents

The homogenized samples were acid-treated with HCl solution (1 M) to completely remove inorganic C before the analysis. The POC and PN contents were determined at Nanjing University using an elemental

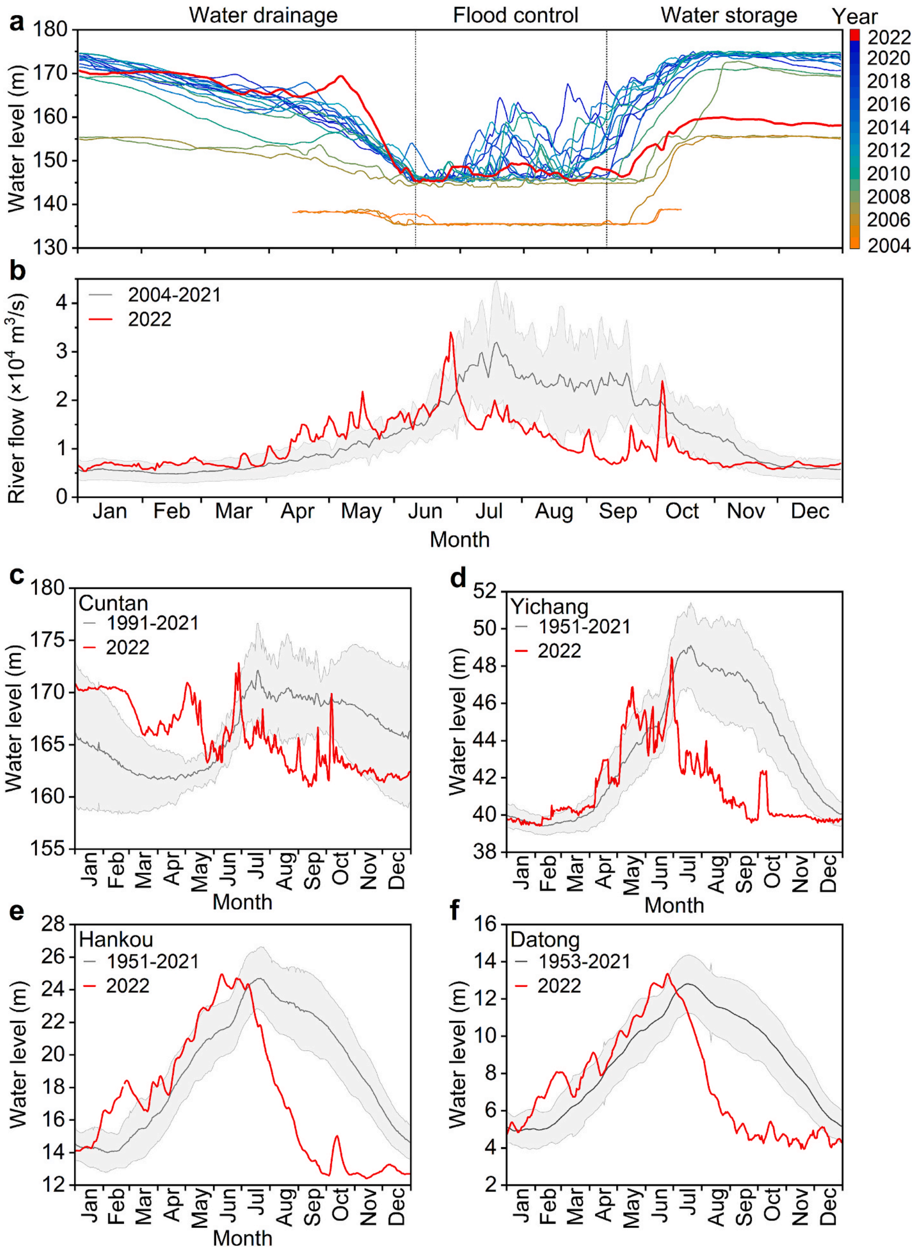

Fig. 2. (a) Water regulation and (b) river flow of the Three Gorges Reservoir since its impoundment. (c-f) Water levels at gauging stations Cuntan (upper reaches), Yichang (middle reaches), Hankou (middle reaches), and Datong (lower reaches), respectively. Modified after Lyu et al. (2025). The data are from the Department of Water Resources of Hubei Province (). Data are presented as means and error bands as the standard deviation.
available at: http://slt.hubei.gov.cn

analyzer (Flash 2000HT, Thermo Fisher Scientific), and the precision of the determination was better than ±0.02 wt% and 0.002 wt%, respectively.

In this study, we quantified the labile fraction of POC as the proportion of LPOC relative to total POC. LPOC was determined using a two-step sulphuric acid hydrolysis procedure, previously developed for characterizing soil organic carbon lability (Belay-Tedla et al., 2009; Oades et al., 1970; Rovira and Vallejo, 2002, 2007). This method separates hydrolysable organic matter based on its biochemical composition, enabling the labile component to be isolated. Hydrolysable carbohydrates represent readily biodegradable compounds, whereas polyphenolic compounds reflect more structurally resistant and slowly decomposing material.

Briefly, 500 mg of the decarbonated sample was hydrolyzed with 20 mL of 2.5 M H_2SO_4 at 105 °C for 30 min. The hydrolysate was recovered by centrifugation and decantation. The residue was washed with 20 mL of pure water, and the washing supernatant was added to the hydrolysate. This hydrolysate was regarded as Labile Pool I. The remaining residue was hydrolyzed with 2 mL of 13 M H_2SO_4 overnight at room temperature under continuous shaking. Afterward, the acid concentration was brought down to 1 M by dilution with pure water, and the sample was hydrolyzed at 105 °C for 3 h with occasional shaking. The second hydrolysate was regarded as Labile Pool II. Labile Pool I and Pool II were summed together to obtain the total Labile Pool. Labile Pool I primarily consists of plant- and microbial-derived polysaccharides (including hemicellulose, starch residues, and microbial cell-wall components), while Labile Pool II is dominated by cellulose. In contrast, the non-hydrolysable fraction contains polyphenolic compounds and other refractory structures that resist microbial breakdown (Oades et al., 1970; Rovira and Vallejo, 2007).

2.4. Stable isotopic value and radiocarbon activity measurements of POC

Stable isotopic compositions were determined at Nanjing University by a mass spectrometer (MAT253, Thermo Fisher Scientific), and the value of δ^{13}C was reported in units per thousand (‰), using standard notation relative to the VPDB (Vienna Pee Dee Belemnite) standard.

Bulk ^{14}C analysis was performed at the Beta Analytic Radiocarbon Dating Laboratory (USA) by AMS. The Δ^{14}C values were corrected for the δ^{13}C fraction, which was measured separately in an IRMS (normalization to $\delta^{13}C = -25$‰) and expressed as conventional radiocarbon age BP (relative to CE 1950) (Mook and Van Der Plicht, 1999; Reimer et al., 2020; Reimer et al., 2004).

2.5. Grain size and suspended sediment concentration (SSC)

The grain size of suspended sediment was measured using a Malvern Mastersizer 2000 laser particle size analyzer. Before measurement, a 1.5 mL sodium metaphosphate dispersion agent was added to each sample, and the samples were then shaken on an overhead shaker for 24 h.

To determine SSC, we measured the dry sediment mass and normalized it by the sampled water volume.

2.6. DNA extraction, PCR amplification, sequencing, and quantitative PCR (qPCR) analysis

Total microbial genomic DNA was extracted from SPM samples using the E.Z.N.A.® soil DNA Kit (Omega Bio-tek, USA) following the manufacturer's instructions. The quality and concentration of DNA were determined by 1.0% agarose gel electrophoresis and a NanoDrop® ND-2000 spectrophotometer (Thermo Scientific Inc., USA).

The gene copy numbers of eukaryotic algae and cyanobacteria in the SPM samples were quantified by qPCR using the primers of 3NDF_V4-euk-R2R and CYA359F_aCYA781R, respectively. Detailed information is provided in Text S1.

2.7. Statistical calculation and analysis

Statistical analysis was done using SPSS (v.24, SPSS Institute, USA). Statistical differences were evaluated with the one-way analysis of variance (ANOVA) at a confidence level of 0.05 for the data that corresponded to the normal distribution, while for the data that did not correspond to the normal distribution (DNA quantity), we used the Kruskal-Wallis test.

A four-endmember mixing model based on Δ^{14}C, δ^{13}C, and PN/POC ratios was used to estimate the proportions of four POC sources (rock, soil, plant, and algae). The PN/POC (N/C) ratio was used to characterize the elemental composition of particulate organic matter, as this formulation avoids the large and highly variable values that can arise when nitrogen-poor organic matter is expressed as POC/PN, thereby providing a more stable basis for source apportionment. Endmember values for the four sources were compiled from studies conducted within the Yangtze River Basin (Table S2). The mass-balance source apportionment was performed in MATLAB (v.R2020b, MathWorks, USA), using the Markov Chain Monte Carlo-driven Bayesian approach (Andersson et al., 2015; Sun et al., 2022). The approach was run with 2 $\times$ 10^5 iterations using a burn-in of 10,000 steps and a data thinning of 100. Andersson et al. (2015) gave the details of this approach, and previous research all used the three-endmember approach. Here, we improved this approach from three-source to four-source apportionment, to analyze the sources of POC more accurately. The model was written as follows:

$$f_{rock} \times \Delta^{14}C_{rock} + f_{soil} \times \Delta^{14}C_{soil} + f_{plant} \times \Delta^{14}C_{plant} + f_{algae} \times \Delta^{14}C_{algae} = \Delta^{14}C_{POC} \quad (1)$$

$$f_{rock} \times \delta^{13}C_{rock} + f_{soil} \times \delta^{13}C_{soil} + f_{plant} \times \delta^{13}C_{plant} + f_{algae} \times \delta^{13}C_{algae} = \delta^{13}C_{POC} \quad (2)$$

$$f_{rock} \times (N/C)_{rock} + f_{soil} \times (N/C)_{soil} + f_{plant} \times (N/C)_{plant} + f_{algae} \times (N/C)_{algae} = (N/C)_{POC} \quad (3)$$

$$f_{rock} + f_{soil} + f_{plant} + f_{algae} = 1 \quad (4)$$

where f_{rock}, f_{soil}, f_{plant}, and f_{algae} represent the fractional proportion of rock-, soil-, plant-, and algae-derived POC, respectively.

Monthly suspended sediment loads and SSC for individual gauging stations in 2021 and 2022 in the Yangtze River were obtained from the *Sediment Communique of Chinese Rivers*, published by the Ministry of Water Resources of China (www.mwr.gov.cn). Based on our observed POC and LPOC contents during 2021–2022, empirical relationships between SSC and POC/LPOC contents were established. These relationships were then combined with sediment load data to estimate basin-scale POC and LPOC fluxes for 2021 and 2022. The same approach was applied to estimate the multi-year average POC flux over the period 2018–2022.

3. Results

3.1. Geochemical characteristics of SPM in different seasons

The POC contents, PN/POC ratios, δ^{13}C values, Δ^{14}C values, LPOC contents, and LPOC/POC ratios of SPM in the mainstem during sampling are shown in Fig. 3. In July 2021, POC contents (Fig. 3a) and PN/POC ratios (Fig. 3b) range from 1.03 wt% to 2.12 wt% (1.36 $\pm$ 0.31 wt% on average) and 0.11 to 0.17 (0.13 $\pm$ 0.01), respectively, and in October 2021, POC contents and PN/POC ratios range from 0.95 wt% to 13.66 wt% (2.47 $\pm$ 3.16 wt%) and 0.12 to 0.17 (0.14 $\pm$ 0.02), respectively. In August 2022 during the extreme drought-heatwave event, POC contents and PN/POC ratios range from 1.27 wt% to 6.53 wt% (2.37 $\pm$ 1.31 wt%) and from 0.15 to 0.18 (0.16 $\pm$ 0.01), respectively, reaching higher values ($F = 14.2$ and 48.1, $P < 0.001$) than those in the summer of 2021, likely illustrating a higher algae-derived POC source during this period (Lamb et al., 2006).

In July 2021, δ^{13}C values (Fig. 3c) range from –26.23‰ to –24.25‰ (–25.62 $\pm$ 0.52‰), in October 2021 from –26.86‰ to –23.82‰ (–25.36 $\pm$ 0.71‰), and in August 2022 from –27.29‰ to –25.27‰ (–26.46 $\pm$ 0.53‰). Δ^{14}C values of POC (Fig. 3d) exhibit strong spatial variations. In July 2021, Δ^{14}C values vary between –455.2‰ and –271.9‰ (–321.7 $\pm$ 47.2‰), corresponding to conventional ^{14}C ages of 2480 to 4810 (3069 $\pm$ 598) years before present (BP). In October 2021, Δ^{14}C values vary between –459.3‰ and –201.6‰ (–267.3 $\pm$ 68.8‰), corresponding to conventional ^{14}C ages of 1740 to 4870 (2466 $\pm$ 828) years BP, which are younger than those in July 2021 ($F = 4.40$, $P = 0.047$), particularly from the TGR to the downstream. In August 2022, Δ^{14}C values vary between –456.6‰ and –219.4‰ (–324.9 $\pm$ 77.0‰), corresponding to conventional ^{14}C ages of 1920 to 4830 (3137 $\pm$ 945) years BP.

In July 2021, LPOC contents (Fig. 3e) range from 0.21 wt% to 0.83 wt% (0.40 $\pm$ 0.17 wt%), in October 2021 from 0.25 wt% to 7.25 wt% (1.02 $\pm$ 1.75 wt%), and in August 2022 from 0.55 wt% to 4.01 wt% (1.20 $\pm$ 0.88 wt%). Herein, LPOC/POC ratios (Fig. 3f) were used to indicate the LPOC proportion of total POC, which in July 2021 varies from 20.3% to 39.0% (28.8 $\pm$ 5.3%), in October 2021 from 24.1% to 53.1% (33.8 $\pm$ 8.0%) with an evident difference in the TGR, and in August 2022 from 34.8% to 61.5% (47.7 $\pm$ 6.7%) with higher values in the whole basin than those in July 2021 and October 2021 ($F = 75.7$ and 41.4, $P < 0.001$).

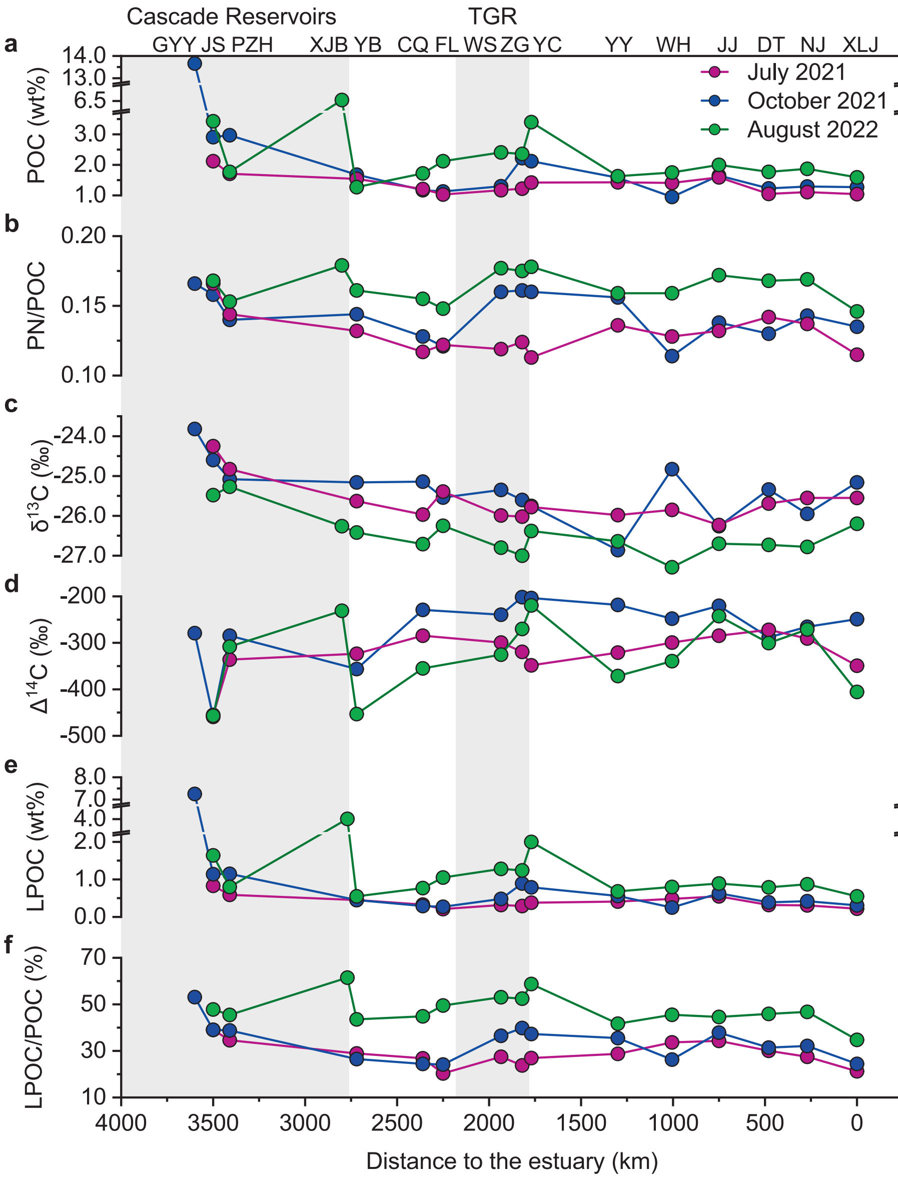

Fig. 3. (a) POC contents, (b) PN/POC ratios (weight/weight), (c) $\delta^{13}C$ values, (d) $\Delta^{14}C$ values, (e) LPOC contents, and (f) LPOC/POC ratios in the mainstem of the Yangtze River. GYY at the Guanyinyan Reservoir was only sampled in October 2021, and XJB at the Xiangjiaba Reservoir was only sampled in August 2022. The two bands represent the cascade reservoirs and TGR. Data points of POC, PN/POC, $\delta^{13}C$ values, LPOC, and LPOC/POC are presented as the mean of duplicate samples. Errors of $\Delta^{14}C$ are 1-sigma counting statistics. Error bars are smaller than symbol sizes and not shown.

3.2. Variation in algae abundance and community composition

DNA-based analyses were used to identify algal taxa and quantify algal abundance in suspended particulate matter from the Yangtze River (Fig. 4). Six algal taxa with relative abundances exceeding 1% were identified, including Bacillariophyta, Chrysophyta, Dinophyta, Chlorophyta, Cryptophyta, and Cyanobacteria.

Algae community composition exhibited seasonal and spatial variability across the three sampling periods. In July 2021 and October 2021, a clear longitudinal shift in dominant algal groups was observed across the TGR, with Bacillariophyta (diatoms) dominating within the reservoir region (stations WS, ZG, and YC), and Cyanobacteria becoming dominant downstream (stations YY to DT) (Fig. 4a, b). In contrast, during the extreme drought–heatwave event in August 2022, Cyanobacteria accounted for the highest proportion among all six taxa across the entire basin ($F = 8.4$, $P < 0.001$; Fig. 4c).

Algae gene quantity ranged from 3.5×10^8 to 1.0×10^{10} copies/g ($3.6 \pm 3.5 \times 10^9$ copies/g on average) in July 2021, and from 8.9×10^8 to 6.4×10^{10} copies/g ($1.5 \pm 1.7 \times 10^{10}$ copies/g) in October 2021. During August 2022, algae gene quantity was significantly higher than in July 2021 ($P < 0.001$), ranging from 2.2×10^9 to 4.0×10^{10} copies/g ($1.6 \pm 1.0 \times 10^{10}$ copies/g). Across all samples, POC and LPOC contents were positively correlated with the gene quantity of algae (Fig. 5a).

4. Discussion

4.1. Source assignment of POC

The organic component of riverine SPM consists of varying contributions from autochthonous (algae) and allochthonous components, with the latter comprising a mixture of modern plant, aged soil, and rock OC from the surrounding basin (Blair and Aller, 2012). Qualitative source attribution based on isotopic and elemental endmembers from previous studies (Fig. 6) reveals seasonal differences in POC composition across the Yangtze River. In July and October 2021 (the normal year), POC occupies an intermediate position between algae and SOM

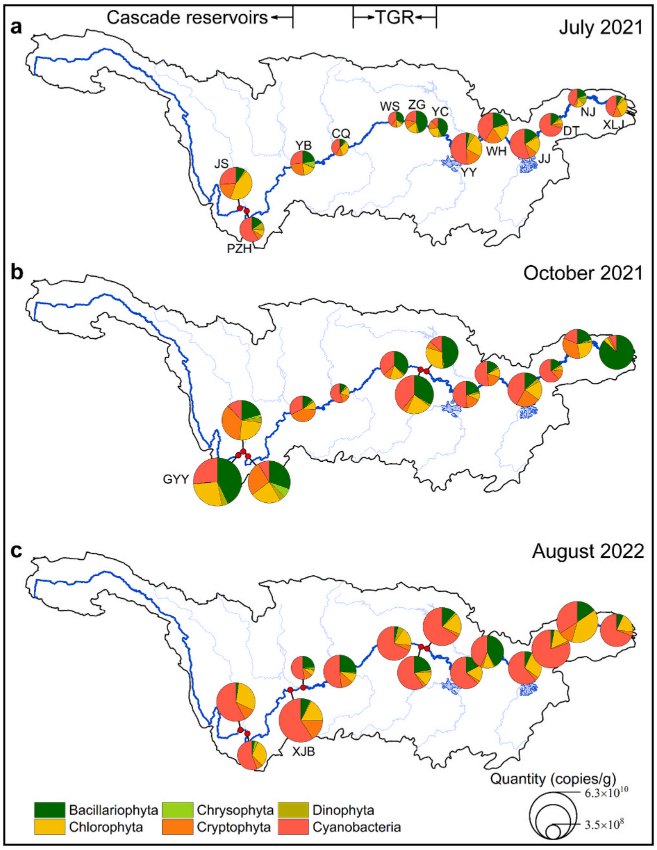

Fig. 4. Distribution of algae in the mainstem of the Yangtze River. Symbols are scaled by the gene quantity of algae and presented as the mean of triplicate samples.

endmembers, indicating mixed contributions from autochthonous and allochthonous contributions. Within these two periods, relatively stronger algal signals are observed during lower water levels, whereas increased SOM influence is apparent under higher discharge conditions, reflecting enhanced soil erosion and lateral inputs. In contrast, samples collected during August 2022, coinciding with the extreme drought–heatwave event, cluster almost exclusively within the algae endmember domain (Fig. 6), indicating a basin-wide dominance of algae-derived POC. This shift reflects the combined effects of suppressed terrestrial inputs due to reduced precipitation and enhanced riverine primary production driven by elevated temperature and prolonged water residence time.

Quantitative source apportionment using the four-endmember mixing model based on region-specific end-member values (Fig. 7) confirms the qualitative patterns inferred from Fig. 6. The model results reveal pronounced seasonal shifts in POC sources, characterized by a substantial increase in algae-derived POC and concurrent decreases in soil- and plant-derived POC during August 2022 relative to July 2021. Together, the qualitative and quantitative analyses indicate that the relative contributions of the four POC sources respond systematically to changes in hydrological conditions.

Moreover, the proportion of LPOC shows a positive relationship with the algae contribution to POC (Fig. 5b), indicating that algae are the primary source of the most rapidly cycling POC fraction. Because algae-derived organic matter is enriched in biochemically labile compounds, shifts toward algae dominance under extreme drought–heatwave conditions are expected to enhance POC lability and accelerate riverine carbon turnover (Davidson and Janssens, 2006; Schädel et al., 2014).

4.2. Water regulation during water storage increases POC lability

In river systems, primary productivity is primarily regulated by energy supply (as light or nutrient inputs) and flow stability, whereas OC decomposition is largely controlled by water residence time (Bernhardt et al., 2022; Catalán et al., 2016). The reservoir-induced river fragmentation in the Yangtze River Basin leads to decreased flow velocity, longer water retention time, and stronger retention of nutrients, which stimulates algae to flourish and OC to accumulate (Kronvang et al., 2005; Ni et al., 2022; Prats et al., 2011; Vörösmarty and Sahagian, 2000; Zhang et al., 2022). Concurrently, damming-induced sediment trapping decreases SSC and alters sediment grain size (Fig. S4), leading to lower turbidity and improved light availability for algae. (Anderson et al., 1997; Chen et al., 2020; Reynolds, 2006). Here both POC and LPOC contents show significant inverse power correlations with SSC (Fig. 5c, d) and no significant correlation with the median grain size of SPM ($P =$ 0.17, 0.15, and 0.10, respectively; two-tailed) during the three periods (July 2021, October 2021, and August 2022), indicating that, of the two sediment properties measured, POC lability is controlled by SSC (SSC and grain size are shown in the Fig. S5).

In addition, water regulation within a year further modifies the hydrological environment (e.g., SSC) and flow stability via different trapping efficiencies (the TGR trapped 75% and 97% of upstream sediment load in July and October 2021, respectively; Fig. S6), which can severely change POC sources and characteristics. In the TGR (stations WS, ZG, and YC in the mid reaches) during the water drainage period represented by July 2021, the higher SSC (Fig. S5b) and water discharge (Fig. S2) are not conducive to algae growth (Figs. 4a and 7d). The strong flow scouring effect downstream of the Three Gorges Dam results in the resuspension of fossil carbon from the riverbed — the erosion downstream of the Three Gorges Dam is worst (MWRC, 1990–2022), which leads to a decrease in POC lability (Fig. 3f) and older POC ages (Fig. 3d) at the stations ZG, YC, and YY in July 2021. With decreasing erosion intensity and increasing algal contributions downstream, POC ages become progressively younger; however, in the estuary, they increase again because strong hydrodynamic processes (e.g., tidal mixing and sediment resuspension) mobilize aged, mineral-bound OC from bottom sediments and subaqueous channels, leading to an apparent aging of bulk POC (Blair and Aller, 2012; Hou et al., 2021; Yu et al., 2024). In the TGR during the water storage period represented by October 2021, river fragmentation is amplified and the water flow is subject to a longer water retention time, in addition to the lower SSC, which leads to significantly higher algae content (11-fold increase in DNA quantity) (Fig. 4b), more algae-derived POC (26 ± 4% increase) (Fig. 7d), higher POC and LPOC content (48 ± 35% and 120 ± 79% increase, respectively) (Fig. 3a and e), and younger POC age (38 ± 13% decrease) (Fig. 3d).

4.3. Increase in POC lability amplified by an extreme drought-heatwave event

Compared to the normal year, the extreme drought-heatwave event provided more energy supply (as light) and led to lower SSC ($F = 8.53$, $P = 0.007$; Fig. S5b) and longer water retention time, as reflected by reduced flow velocity (Fig. 2b). These conditions jointly promoted increases in POC content, algae-derived POC, and POC lability over that in July 2021 and October 2021 (Figs. 3a, f, 4, and 7d). Notably, the contents of POC, LPOC, and algae were higher across the whole basin despite elevated temperatures that would otherwise accelerate OC degradation, suggesting that water retention time played a more important role in OC degradation rate (Catalán et al., 2016).

Specifically, relative to July 2021, the proportions of algae-derived POC and LPOC increased by 19 ± 11% and 18 ± 8% in the whole basin, respectively, with higher increases of 34 ± 7% and 29 ± 3% in the TGR (compared with the non-TGR areas; $F = 11.66$ and 15.46, $P = 0.006$ and 0.002), respectively; this spatial contrast reflects the combined

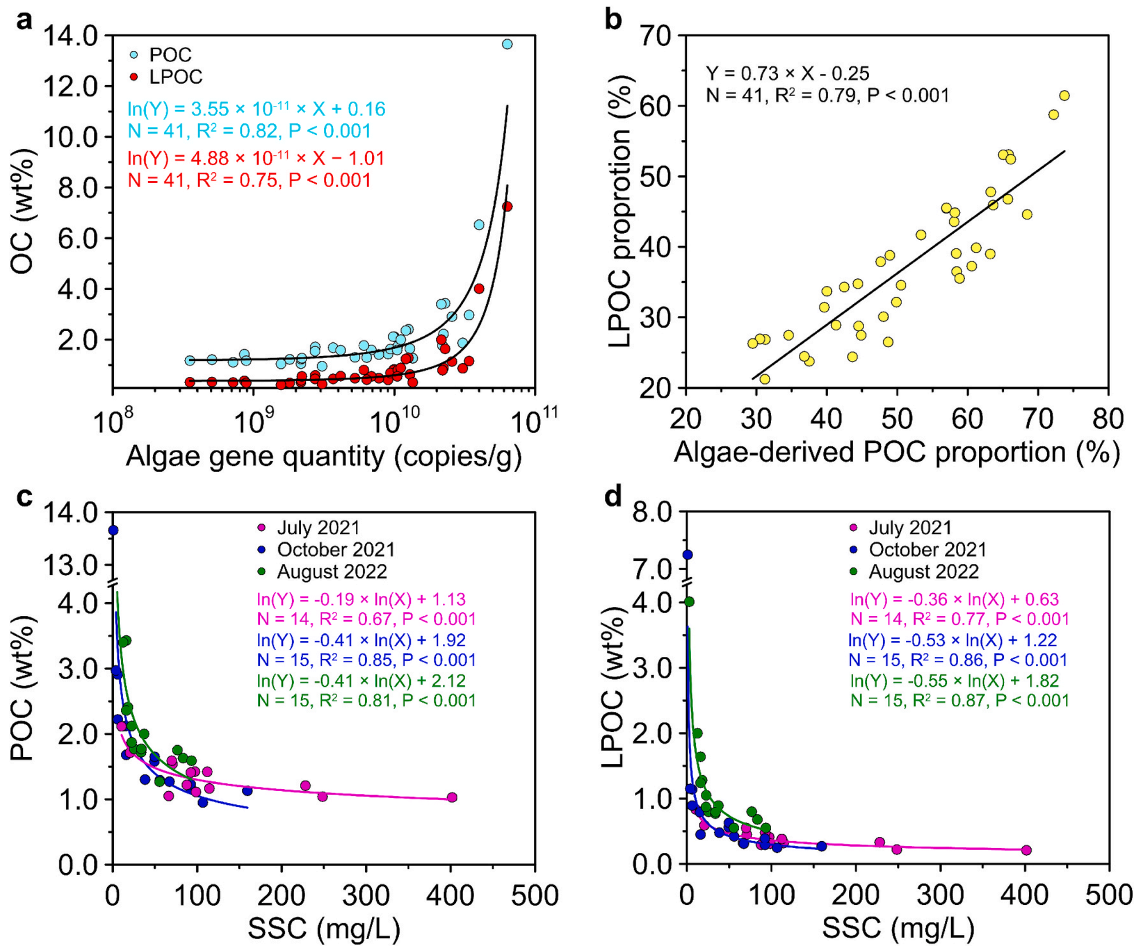

Fig. 5. Correlation of (a) POC content and algae gene quantity, modified after Lyu et al. (2025), (b) LPOC proportion and algae-derived POC proportion, (c) POC content and SSC, and (d) LPOC content and SSC. The algae gene quantity in (a) is from DNA analysis, the LPOC proportion in (b) is from LPOC/POC ratios, and the algae-derived POC proportion in (b) is from the endmember analysis. Error bars are smaller than symbol sizes and not shown.

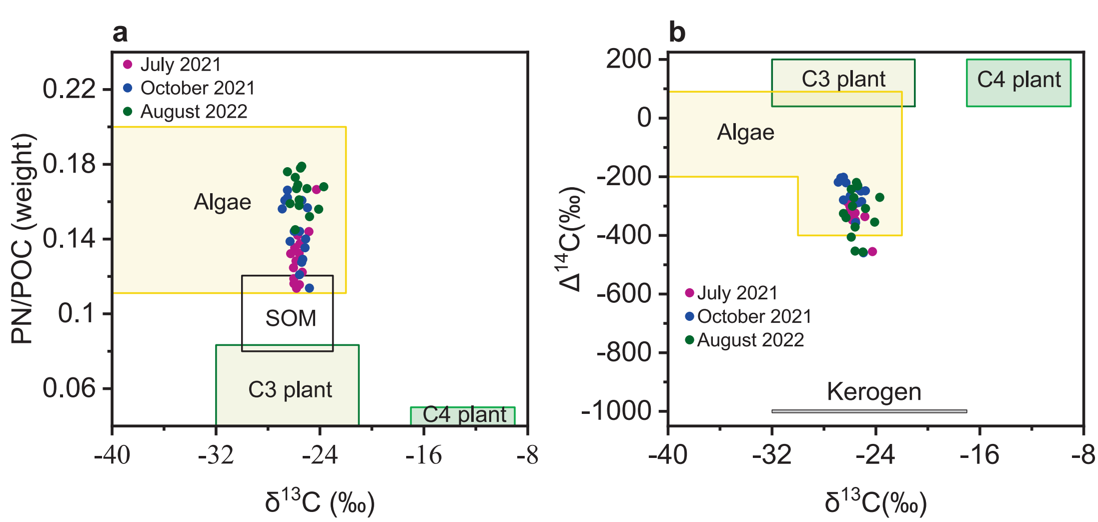

Fig. 6. Diagram indicating the provenance of samples based on (a) POC/PN and $\delta^{13}C$ (SOM = soil organic matter; modified after Goni et al. (2008) and Lamb et al. (2006), and references therein), and (b) $\delta^{13}C$ and $\Delta^{14}C$ (modified after Marwick et al. (2015)). Data points are presented as the mean of duplicate samples. Error bars are smaller than symbol sizes and not shown.

effect of the extreme drought-heatwave event and damming on increasing POC lability. In contrast, POC lability in the upstream cascade reservoir system (stations JS and PZH) showed little difference between July 2021, October 2021, and August 2022 (Figs. 3f and 7d), despite the occurrence of the extreme drought-heatwave event. This muted response can be attributed to persistently low suspended sediment concentrations throughout the year (<30 mg/L at the gauging station Panzhihua), resulting from the high and relatively constant trapping

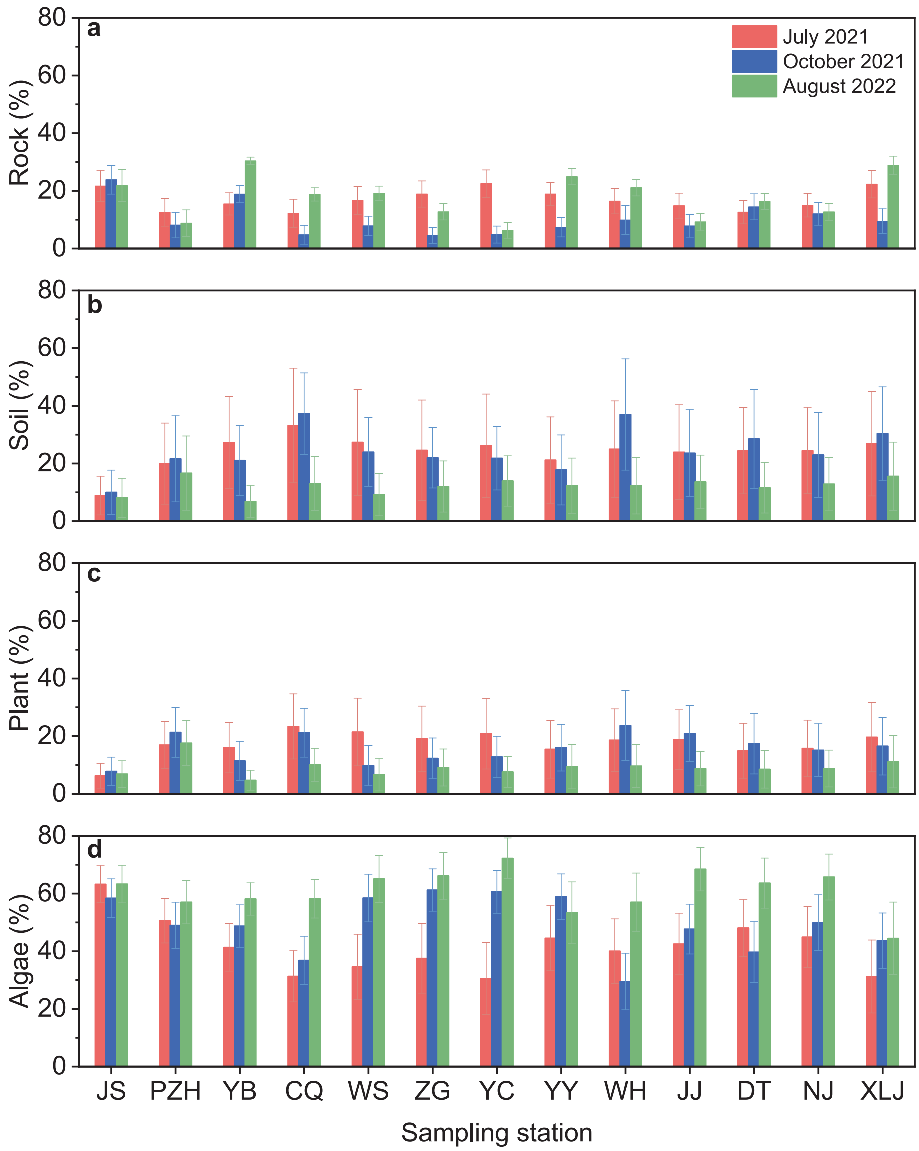

Fig. 7. Sources of POC derived from (a) rock, (b) soil, (c) plant, and (d) algae. Proportions are estimated by using the Bayesian source apportionment of POC based on PN/POC, $\delta^{13}C$, and $\Delta^{14}C$; error bars represent the end-member uncertainties for each point.

efficiency of the upstream cascade reservoirs.

The comparison between the upstream cascade reservoirs and the Three Gorges Reservoir region highlights a clear spatial contrast in the combined effects of damming and extreme climate. While dam regulation in the cascade reservoirs already imposes a stable low-SSC regime, limiting further climate-induced changes in POC lability, extreme drought–heatwave conditions in the TGR substantially altered hydrological and sedimentary conditions, leading to a pronounced increase in algae-derived and labile POC. This contrast demonstrates that the combined effect of damming and extreme climate on POC lability is stronger where climatic extremes induce additional hydrological shifts beyond baseline dam regulation.

Given that reservoirs are preferential sites of OC accumulation, the increased POC lability may severely affect carbon storage in the Yangtze River Basin and other major river basins (Maavara et al., 2017). Simultaneously, the changed hydrological conditions (e.g., higher temperature and lower water level) caused by the extreme drought-heatwave event led to evident changes in biomass and successions of dominant algae taxa (Fig. 4), which may affect ecological stability in the Yangtze River Basin and other major river systems (Li et al., 2022). In particular, the increased dominance of cyanobacteria under such warm and stagnant conditions has been widely associated with elevated risks of harmful algal blooms (HABs), including the potential release of toxins such as microcystins, which can threaten drinking-water safety and impair ecosystem services (Huisman et al., 2018; Paerl and Otten, 2013). Although not directly evaluated in this study, these potential risks highlight the broader implications of climate-induced hydrological extremes for water security in large river basins.

Owing to the extreme drought-heatwave event in 2022, the annual sediment export from the Yangtze River to the East China Sea experienced a substantial decline, decreasing from an average value of 112 ± 31 Tg/yr in previous years (2017–2021) to 67 Tg/yr in 2022. Given that the POC flux from the Yangtze River into the sea was not measured in 2022, we used the relationship between SSC and POC content to estimate it (Text S2). In 2021 with normal water discharge and sediment loads, the estimated POC flux from the Yangtze River to the sea is 1.22 ± 0.04 Tg C/yr, which is very similar to the observed 1.2 Tg C/yr (Lyu et al., 2023), demonstrating the reliability of the estimation method. Compared with 2021, the estimated annual export POC flux to the sea in 2022 is 0.86 ± 0.06 Tg C/yr, and is thus decreased by 29 ± 6%, whereas the LPOC proportion of the export POC increases by 15 ± 4% during the whole year. This shift is consistent with the hydro-climatic conditions in

2022, when extremely low precipitation reduced soil erosion and thus limited allochthonous POC delivery from slopes, whereas prolonged high-temperature and stable hydrodynamic conditions favored algal production in the mainstem. As a result, autochthonous and more labile POC contributed proportionally more to the exported POC pool. Based on the above relationship, we estimate the annual POC flux, annual LPOC flux, and the difference in the LPOC proportion of the annual POC flux between the normal and extreme drought-heatwave years in the whole basin. These results highlight both the strong trapping effect of the TGR on POC and LPOC fluxes (Fig. 8a, b) and the basin-wide enhancement of LPOC proportion associated with the extreme drought–heatwave event in 2022 (Fig. 8c).

4.4. Global implications for carbon cycling in major river systems

In the Yangtze River Basin, the source-to-sink system of POC is experiencing substantial transformations driven by dam trapping, from the initial POC transit channel to the present four source-to-sink subsystems (Figs. S7 and S8). The construction of dams in the Yangtze River not only reduced the export POC flux, but also increased the relative contribution of algal-derived POC, thereby potentially altering its lability (Lyu et al., 2023; Fig. 9a). On this basis, intra-annual water regulation further modifies both the sources and lability of POC, with particularly pronounced effects observed within the reservoir region (Fig. 9b). Superimposed on these anthropogenic influences, the occurrence of the extreme drought-heatwave event intensifies the alterations in POC characteristics and fluxes, leading to more complex and variable biogeochemical responses (Fig. 9c).

Although there is a lack of observation data for all global rivers, the changes in POC source, lability, and flux due to water regulation and extreme weather events likely apply to other rivers worldwide. The lability of POC, which refers to its rate of decomposition and transformation within river systems, directly influences the carbon flux in these systems. Higher lability indicates that organic carbon is more readily decomposed by microbes, thereby increasing carbon release and transfer. Such enhanced microbial mineralization of labile organic carbon is identified as a key driver of greenhouse gas emissions from inland waters, which act as active components of the global carbon cycle (Cole et al., 2007). This change not only affects the carbon cycle within the local river system but also has potential implications for regional and global carbon fluxes. In addition, reservoirs trap more soil-derived POC and contribute algae-derived POC (Fig. 7), and the source of export POC is changing from soil-dominated to algae-dominated (Lyu et al., 2023), which leads to more labile POC. As a foundational step toward elucidating the impacts of POC lability changes on the global carbon cycle, it is essential to examine variations in POC fluxes across global river systems before and after dam construction.

Given that global damming has led to a substantial reduction in sediment flux—49% of pre-dam conditions (Dethier et al., 2022)—we collated available sediment load and POC flux data from global major rivers (Table S3). These data reveal a significant linear relationship between sediment load and POC flux ($R^2 = 0.89$, $P < 0.001$, $n = 180$, Fig. S9), and a similar linear dependence between sediment load and POC flux has also been reported by Galy (2015). Based on this relationship, the global decline in sediment discharge caused by damming suggests an approximately proportional reduction in riverine POC export; thus, the contemporary global POC flux is expected to be roughly 49% of its pre-dam conditions. Furthermore, we illustrated the spatial distribution of dam-induced reductions in POC fluxes across major rivers worldwide (Fig. 9d), using documented declines in sediment loads (Table S4). Because this approach is based on a conceptual scaling rather than detailed global budgeting, we refrain from reporting specific POC flux values. More comprehensive datasets and refined modeling efforts will be required for quantitatively robust post-dam global POC flux estimates. Nonetheless, this assessment highlights the substantial implications of sediment trapping for global POC flux.

While POC flux declines, damming enhances the riverine primary productivity, and here we find that water storage within a year further increases the lability of POC, and that extreme weather events amplify this, which consequently necessitates a re-evaluation of the resulting ecological and environmental effects. Most large rivers worldwide are being (or will be) affected by the water regulation of dams, such as the Amazon, the Ganges-Bangladesh, the Mekong, the Mississippi, the Nile, and the Yellow Rivers (Hecht et al., 2019; Liu et al., 2022; Maavara et al., 2017; Sadaoui et al., 2018), and dam construction is still increasing (Dethier et al., 2022). Simultaneously, the probability of extreme drought-heatwave events is increasing due to climate change (Fischer et al., 2021; Perkins-Kirkpatrick and Lewis, 2020), and the 2022-like events could occur once every 8.5 years, rather than the current possibility of once in every 76,000 years (Hua et al., 2023). Compared to droughts, climate change is also projected to intensify extreme precipitation and flooding events, which have contrasting effects on riverine carbon dynamics: extreme floods often mobilize large quantities of soil organic matter and suspended sediment, and thereby substantially increase OC export (Clark et al., 2022; Dalzell et al., 2005), whereas drought–heatwaves tend to reduce sediment transport and favour riverine production of labile OC. Moreover, water regulation and extreme weather events alter algal communities (Fig. 4), which can affect the ecology stability and carbon cycling process in rivers and coastal areas (Deemer et al., 2022; Li et al., 2022). Accordingly, as damming and extreme weather events increasingly combine to impose more frequent and severe disturbances on river systems, estimating POC flux with varying compositions under these conditions becomes essential, thereby warranting a reassessment of the contribution of global rivers to the global carbon budget.

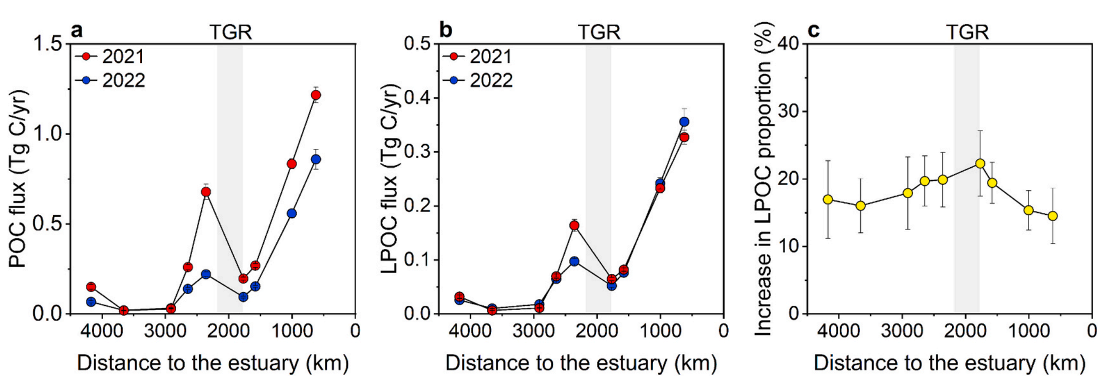

Fig. 8. (a) Annual POC flux, (b) annual LPOC flux, and the increase in the LPOC proportion of the annual POC flux in the mainstem of the Yangtze River (c) from the normal year (2021) to the extreme (2022) year. The POC fluxes are estimated based on the sediment loads at gauging stations and the relationship between SSC and POC contents. Error bars represent the uncertainties of each point at a 95% confidence interval.

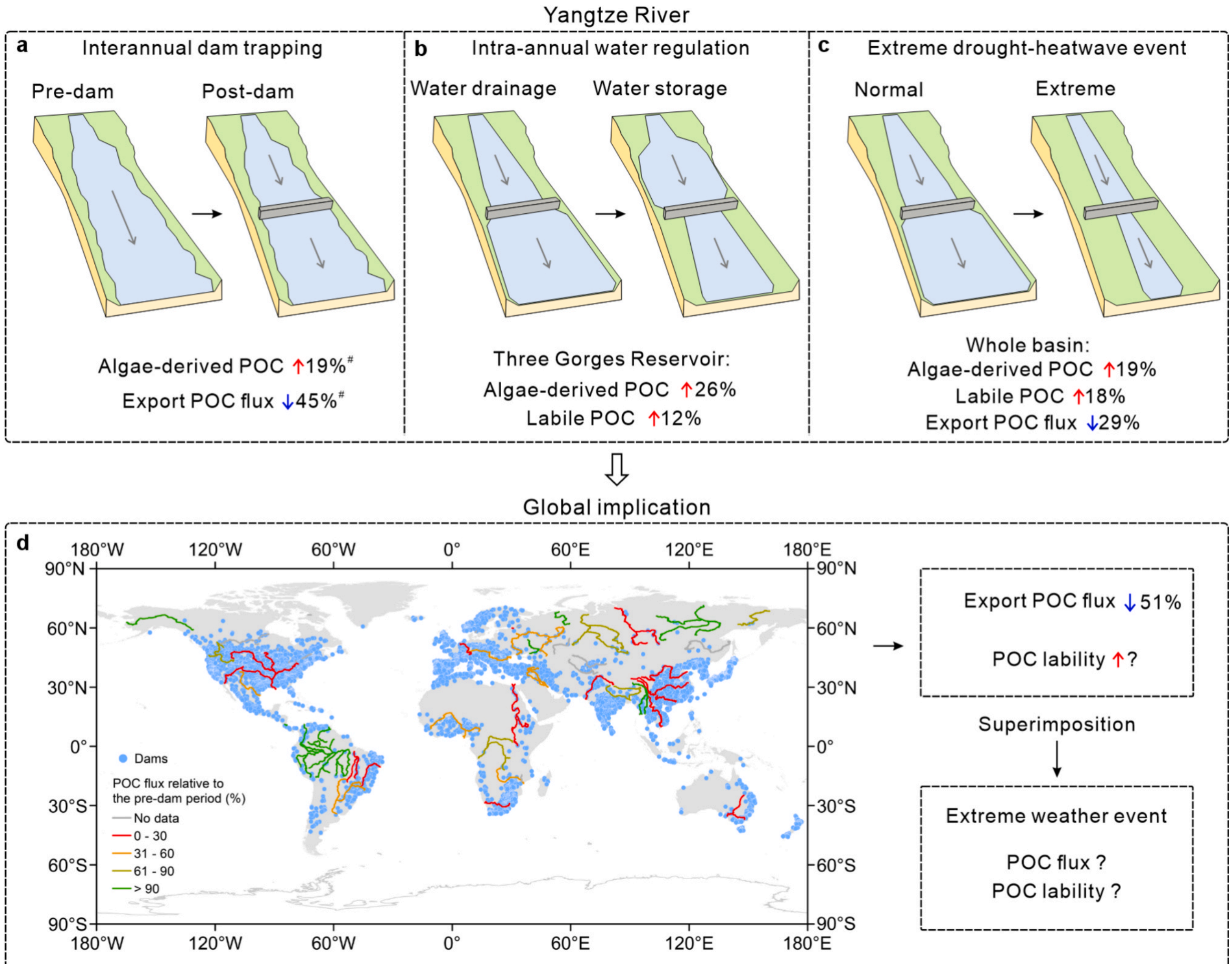

Fig. 9. (a) Impact of interannual dam trapping on the export POC source and flux; # The data are estimated from Lyu et al. (2023). (b) Impact of intra-annual water regulation on the POC source and lability within the Three Gorges Reservoir. (c) Impact of the extreme drought-heatwave event on the POC source and lability within the whole basin, and the impact on the export POC flux. (d) Global distribution of riverine POC flux affected by dams, and changes in global POC flux and lability; dam positions are from the Global Reservoirs and Dams (GRanD) database (https://www.globaldamwatch.org).

5. Conclusions

By using the Yangtze River as an example, we explore the impact of water regulation and an extreme drought-heatwave event on the source, lability and export flux of POC for the first time. We find that in a normal year, water storage by the TGR increases the proportion of algae-derived POC and leads to a higher proportion of labile POC and younger POC ages, while the extreme drought-heatwave event further amplifies this effect and increases the proportion of labile POC by 18 ± 8% in the whole basin, with a greater increase by 29 ± 3% in the TGR, simultaneously resulting in a 29 ± 6% reduction in export POC flux to the East China Sea. By using our findings from the Yangtze River, we estimate that the global riverine export POC flux decreases from pre-dam 190 ± 5 Tg C/yr to post-dam 97 ± 48 Tg C/yr. Globally we assert that more frequent extreme drought-heatwave events will compound the effects of damming, resulting in an increasingly labile and thus more readily remineralized riverine POC source and a decreasing export POC flux into the near-shore environment, which severely affects the global carbon budget and the global carbon cycle.

Data availability

The datasets are deposited in Zenodo and can be found via https://doi.org/10.5281/zenodo.18923965.

CRediT authorship contribution statement

Jixuan Lyu: Writing – original draft, Investigation, Formal analysis, Data curation, Conceptualization. **Caroline L. Peacock:** Writing – review & editing, Supervision. **Yifan Zhang:** Methodology, Investigation. **Tao Liu:** Investigation. **Yong Shi:** Investigation, Conceptualization. **Xiaomei Xu:** Data curation. **Shengjing Liu:** Investigation. **Yubing Qu:** Methodology. **Shuo Zhang:** Investigation. **Guang Yang:** Visualization, Investigation. **Dong Peng:** Methodology, Investigation. **Chonghao Chen:** Investigation. **Xin Zhou:** Visualization. **Yanxu Zhang:** Supervision. **Jianhua Gao:** Supervision, Project administration, Funding acquisition.

Declaration of competing interest

The authors declare that they have no known competing financial interests or personal relationships that could have appeared to influence the work reported in this paper.

Acknowledgments

This research was funded by National Natural Science Foundation of China (42506236, 42276170, 42293261, and 42106158), Fundamental Research Funds for the Central Universities (14380100), and Basic Research Program of Jiangsu (BK20251202).

Appendix A. Supplementary material

The supplementary material associated with this article provides detailed methodological descriptions, hydrological records, and geochemical datasets that support the interpretations discussed in the main text. Text S1 details the protocols for DNA extraction, PCR amplification, and quantitative PCR (qPCR) analysis used to identify and quantify eukaryotes and cyanobacteria within the suspended particulate matter. Figs. S1–S5 and S8 present comprehensive spatiotemporal data on water discharge, sediment load, suspended sediment concentration (SSC), and grain size along the Yangtze River, including specific observations during the 2022 extreme drought-heatwave event. The trapping effects of cascade dams and the Three Gorges Reservoir on sediment and the resulting changes to the particulate organic carbon (POC) source-to-sink system are illustrated in Figs. S6–S7 and Table S1. Table S2 lists the endmember values of Δ^{14}C, δ^{13}C, and N/C ratios for various POC sources used in the study. Finally, to contextualize the findings globally, Fig. S9, Table S3, and Table S4 compile data on POC fluxes, sediment loads, and dam-induced sediment reductions from major rivers worldwide. Supplementary material to this article can be found online at https://doi.org/10.1016/j.gca.2026.03.056.

References

Anderson, J.M., Park, Y.I., Chow, W., 1997. Photoinactivation and photoprotection of photosystem II in nature. Physiol. Plant. 100 (2), 214–223.
Andersson, A., Deng, J., Du, K., Zheng, M., Yan, C., Sköld, M., Gustafsson, O.R., 2015. Regionally-varying combustion sources of the January 2013 severe haze events over eastern China. Environ. Sci. Technol. 49 (4), 2038–2043.
Belay-Tedla, A., Zhou, X., Su, B., Wan, S., Luo, Y., 2009. Labile, recalcitrant, and microbial carbon and nitrogen pools of a tallgrass prairie soil in the US Great Plains subjected to experimental warming and clipping. Soil Biol. Biochem. 41 (1), 110–116.
Bernhardt, E.S., Savoy, P., Vlah, M.J., Appling, A.P., Koenig, L.E., Hall Jr, R.O., Arroita, M., Blaszczak, J.R., Carter, A.M., Cohen, M., 2022. Light and flow regimes regulate the metabolism of rivers. Proc. Natl. Acad. Sci. 119 (8), e2121976119.
Best, J., 2019. Anthropogenic stresses on the world's big rivers. Nat. Geosci. 12 (1), 7–21.
Blair, N.E., Aller, R.C., 2012. The fate of terrestrial organic carbon in the marine environment. Ann. Rev. Mar. Sci. 4 (1), 401–423.
Catalán, N., Marcé, R., Kothawala, D.N., Tranvik, L.J., 2016. Organic carbon decomposition rates controlled by water retention time across inland waters. Nat. Geosci. 9 (7), 501–504.
Chen, Q., Shi, W., Huisman, J., Maberly, S.C., Zhang, J., Yu, J., Chen, Y., Tonina, D., Yi, Q., 2020. Hydropower reservoirs on the upper Mekong River modify nutrient bioavailability downstream. Natl. Sci. Rev. 7 (9), 1449–1457.
Clark, K.E., Stallard, R., Murphy, S.F., Scholl, M.A., González, G., Plante, A.F., McDowell, W.H., 2022. Extreme rainstorms drive exceptional organic carbon export from forested humid-tropical rivers in Puerto Rico. Nat. Commun. 13 (1), 2058.
Cole, J.J., Prairie, Y.T., Caraco, N.F., McDowell, W.H., Tranvik, L.J., Striegl, R.G., Duarte, C.M., Kortelainen, P., Downing, J.A., Middelburg, J.J., 2007. Plumbing the global carbon cycle: integrating inland waters into the terrestrial carbon budget. Ecosystems 10 (1), 172–185.
Coronese, M., Lamperti, F., Keller, K., Chiaromonte, F., Roventini, A., 2019. Evidence for sharp increase in the economic damages of extreme natural disasters. Proc. Natl. Acad. Sci. 116 (43), 21450–21455.
Dalzell, B.J., Filley, T.R., Harbor, J.M., 2005. Flood pulse influences on terrestrial organic matter export from an agricultural watershed. J. Geophys. Res. Biogeo. 110 (G2).
Davidson, E.A., Janssens, I.A., 2006. Temperature sensitivity of soil carbon decomposition and feedbacks to climate change. Nature 440 (7081), 165–173.
Deemer, B.R., Yackulic, C.B., Hall Jr, R.O., Dodrill, M.J., Kennedy, T.A., Muehlbauer, J. D., Topping, D.J., Voichick, N., Yard, M.D., 2022. Experimental reductions in subdaily flow fluctuations increased gross primary productivity for 425 river kilometers downstream. PNAS Nexus 1 (3), pgac094.
Derrien, M., Brogi, S.R., Gonçalves-Araujo, R., 2019. Characterization of aquatic organic matter: assessment, perspectives and research priorities. Water Res. 163, 114908.
Dethier, E.N., Renshaw, C.E., Magilligan, F.J., 2022. Rapid changes to global river suspended sediment flux by humans. Science 376 (6600), 1447–1452.
Fischer, E., Sippel, S., Knutti, R., 2021. Increasing probability of record-shattering climate extremes. Nat. Clim. Chang. 11 (8), 689–695.
Galy, V., Beyssac, O., France-Lanord, C., Eglinton, T., 2008. Recycling of graphite during Himalayan erosion: a geological stabilization of carbon in the crust. Science 322 (5903), 943–945.
Galy, V., Peucker-Ehrenbrink, B., Eglinton, T., 2015. Global carbon export from the terrestrial biosphere controlled by erosion. Nature 521 (7551), 204–207.
Goni, M.A., Monacci, N., Gisewhite, R., Crockett, J., Nittrouer, C., Ogston, A., Alin, S.R., Aalto, R., 2008. Terrigenous organic matter in sediments from the Fly River delta-clinoform system (Papua New Guinea). J. Geophys. Res. Earth 113 (F1).
Grill, G., Lehner, B., Lumsdon, A.E., MacDonald, G.K., Zarfl, C., Liermann, C.R., 2015. An index-based framework for assessing patterns and trends in river fragmentation and flow regulation by global dams at multiple scales. Environ. Res. Lett. 10 (1), 015001.
Grill, G., Lehner, B., Thieme, M., Geenen, B., Tickner, D., Antonelli, F., Babu, S., Borrelli, P., Cheng, L., Crochetiere, H., 2019. Mapping the world's free-flowing rivers. Nature 569 (7755), 215–221.
Hecht, J.S., Lacombe, G., Arias, M.E., Dang, T.D., Piman, T., 2019. Hydropower dams of the Mekong River basin: a review of their hydrological impacts. J. Hydrol. 568, 285–300.
Hou, P., Eglinton, T.I., Yu, M., Montluçon, D.B., Haghipour, N., Zhang, H., Jin, G.E., Zhao, M., 2021. Degradation and aging of terrestrial organic carbon within estuaries: biogeochemical and environmental implications. Environ. Sci. Technol. 55 (15), 10852–10861.
Hua, W., Dai, A., Qin, M., Hu, Y., Cui, Y., 2023. How unexpected was the 2022 summertime heat extremes in the middle reaches of the Yangtze River? Geophys. Res. Lett. 50 (16), e2023GL104269.
Huisman, J., Codd, G.A., Paerl, H.W., Ibelings, B.W., Verspagen, J.M., Visser, P.M., 2018. Cyanobacterial blooms. Nat. Rev. Microbiol. 16 (8), 471–483.
Kennedy, J., 2022. WMO Provisional State of the Global Climate 2022.
Kronvang, B., Hezlar, J., Jensen, J., Behrendt, H., Andersen, T., Arheimer, B., Venohr, M., Hoffman, C., Nielsen, C., 2005. EUROHARP 9-2004. Nutrient Retention Handbook.
Lamb, A.L., Wilson, G.P., Leng, M.J., 2006. A review of coastal palaeoclimate and relative sea-level reconstructions using δ13C and C/N ratios in organic material. Earth Sci. Rev. 75 (1–4), 29–57.
Li, F., Guo, F., Gao, W., Cai, Y., Zhang, Y., Yang, Z., 2022. Environmental DNA biomonitoring reveals the interactive effects of dams and nutrient enrichment on aquatic multitrophic communities. Environ. Sci. Technol. 56 (23), 16952–16963.
Li, G., Wang, X.T., Yang, Z., Mao, C., West, A.J., Ji, J., 2015. Dam-triggered organic carbon sequestration makes the Changjiang (Yangtze) river basin (China) a significant carbon sink. J. Geophys. Res. Biogeo. 120 (1), 39–53.
Li, N., Wang, L., Zeng, C., Wang, D., Liu, D., Wu, X., 2016. Variations of runoff and sediment load in the middle and lower reaches of the Yangtze River, China (1950-2013). PLoS One 11 (8), e0160154.
Liu, D., Bai, Y., He, X., Pan, D., Chen, C.-T.-A., Li, T., Xu, Y., Gong, C., Zhang, L., 2019. Satellite-derived particulate organic carbon flux in the Changjiang River through different stages of the three Gorges Dam. Remote Sens. Environ. 223, 154–165.
Liu, D., Tian, L., Jiang, X., Wu, H., Yu, S., 2022. Human activities changed organic carbon transport in Chinese rivers during 2004-2018. Water Res. 222, 118872.
Lu, T., Wang, H., Hu, L., Wu, X., Bi, N., Dang, Y., Assavapanuvat, P., Bianchi, T.S., 2023. Dynamic transport of particulate organic carbon in the Yellow River during dam-orientated water-sediment regulation. Mar. Geol. 460, 107054.
Ludwig, W., Probst, J.L., Kempe, S., 1996. Predicting the oceanic input of organic carbon by continental erosion. Global Biogeochem. Cycles 10 (1), 23–41.
Lyu, J., Shi, Y., Liu, T., Xu, X., Liu, S., Yang, G., Peng, D., Qu, Y., Zhang, S., Chen, C., 2025. Extreme drought-heatwave events threaten the biodiversity and stability of aquatic plankton communities in the Yangtze River ecosystems. Commun. Earth Environ. 6 (1), 171.
Lyu, J., Shi, Y., Zhang, S., Liu, S., Liu, T., Xu, X., Yang, G., Gao, J., 2023. The reservoirs gradually changed the distribution, source, and flux of particulate organic carbon within the Changjiang River catchment. J. Hydrol. 623, 129808.
Maavara, T., Lauerwald, R., Regnier, P., Van Cappellen, P., 2017. Global perturbation of organic carbon cycling by river damming. Nat. Commun. 8 (1), 15347.
Mallapaty, S., 2022. China's extreme weather challenges scientists studying it. Nature 609 (7929), 888.
Marwick, T.R., Tamooh, F., Teodoru, C.R., Borges, A.V., Darchambeau, F., Bouillon, S., 2015. The age of river-transported carbon: a global perspective. Global Biogeochem. Cycles 29 (2), 122–137.
Mook, W.G., Van Der Plicht, J., 1999. Reporting 14C activities and concentrations. Radiocarbon 41 (3), 227–239.
MWRC, 1990–2022.. Sediment Communique of Chinese Rivers. China Water & Power Press, Beijing.
Ni, J., Wang, H., Ma, T., Huang, R., Ciais, P., Li, Z., Yue, Y., Chen, J., Li, B., Wang, Y., 2022. Three Gorges Dam: friend or foe of riverine greenhouse gases? Natl. Sci. Rev. 9 (6), nwac013.
Oades, J., Kirkman, M., Wagner, G., 1970. The use of gas-liquid chromatography for the determination of sugars extracted from soils by sulfuric acid. Soil Sci. Soc. Am. J. 34 (2), 230–235.
Paerl, H.W., Otten, T.G., 2013. Harmful cyanobacterial blooms: causes, consequences, and controls. Microb. Ecol. 65 (4), 995–1010.
Perkins-Kirkpatrick, S., Lewis, S., 2020. Increasing trends in regional heatwaves. Nat. Commun. 11 (1), 3357.
Prats, J., Armengol, J., Marcé, R., Sánchez-Juny, M., Dolz, J., 2011. Dams and reservoirs in the lower Ebro River and its effects on the river thermal cycle. Ebro River Basin 77–95.
Regnier, P., Resplandy, L., Najjar, R.G., Ciais, P., 2022. The land-to-ocean loops of the global carbon cycle. Nature 603 (7901), 401–410.

Reimer, P.J., Austin, W.E., Bard, E., Bayliss, A., Blackwell, P.G., Ramsey, C.B., Butzin, M., Cheng, H., Edwards, R.L., Friedrich, M., 2020. The IntCal20 Northern Hemisphere radiocarbon age calibration curve (0–55 cal kBP). Radiocarbon 62 (4), 725–757.
Reimer, P.J., Brown, T.A., Reimer, R.W., 2004. Discussion: reporting and calibration of post-bomb 14C data. Radiocarbon 46 (3), 1299–1304.
Repasch, M., Scheingross, J.S., Hovius, N., Lupker, M., Wittmann, H., Haghipour, N., Gröcke, D.R., Orfeo, O., Eglinton, T.I., Sachse, D., 2021. Fluvial organic carbon cycling regulated by sediment transit time and mineral protection. Nat. Geosci. 14 (11), 842–848.
Reynolds, C.S., 2006. The Ecology of Phytoplankton. Cambridge University Press.
Rovira, P., Vallejo, V.R., 2002. Labile and recalcitrant pools of carbon and nitrogen in organic matter decomposing at different depths in soil: an acid hydrolysis approach. Geoderma 107 (1–2), 109–141.
Rovira, P., Vallejo, V.R., 2007. Labile, recalcitrant, and inert organic matter in Mediterranean forest soils. Soil Biol. Biochem. 39 (1), 202–215.
Russo, S., Dosio, A., Graversen, R.G., Sillmann, J., Carrao, H., Dunbar, M.B., Singleton, A., Montagna, P., Barbola, P., Vogt;, J.V., 2014. Magnitude of extreme heat waves in present climate and their projection in a warming world. J. Geophys. Res. Atmos. 119 (22), 12,500–512,512.
Sadaoui, M., Ludwig, W., Bourrin, F., Romero, E., 2018. The impact of reservoir construction on riverine sediment and carbon fluxes to the Mediterranean Sea. Prog. Oceanogr. 163, 94–111.
Schädel, C., Schuur, E.A., Bracho, R., Elberling, B., Knoblauch, C., Lee, H., Luo, Y., Shaver, G.R., Turetsky, M.R., 2014. Circumpolar assessment of permafrost C quality and its vulnerability over time using long-term incubation data. Glob. Chang. Biol. 20 (2), 641–652.
Sun, X., Fan, D., Hu, L., Yang, Z., Guo, Z., 2022. Oxidation of petrogenic organic carbon in a large river-dominated estuary. Geochim. Cosmochim. Acta 338, 136–153.
Syvitski, J.P., Vörösmarty, C.J., Kettner, A.J., Green, P., 2005. Impact of humans on the flux of terrestrial sediment to the global coastal ocean. Science 308 (5720), 376–380.
Tessler, Z.D., Vörösmarty, C.J., Grossberg, M., Gladkova, I., Aizenman, H., Syvitski, J.P., Foufoula-Georgiou, E., 2015. Profiling risk and sustainability in coastal deltas of the world. Science 349 (6248), 638–643.
Teuling, A.J., 2018. A hot future for European droughts. Nat. Clim. Chang. 8 (5), 364–365.
Tian, Y.Q., Yu, Q., Feig, A.D., Ye, C., Blunden, A., 2013. Effects of climate and land-surface processes on terrestrial dissolved organic carbon export to major US coastal rivers. Ecol. Eng. 54, 192–201.
Toreti, A., Bavera, D., Acosta Navarro, J., Cammalleri, C., de Jager, A., Di Ciollo, C., Hrast Essenfelder, A., Maetens, W., Magni, D., Masante, D., 2022. Drought in Europe august 2022. Publications Office of the European Union, Luxembourg 10, 264241.
Vörösmarty, C.J., Sahagian, D., 2000. Anthropogenic disturbance of the terrestrial water cycle. Bioscience 50 (9), 753–765.
Wang, C., Hao, Z., Gao, J., Feng, Z., Ding, Y., Zhang, C., Zou, X., 2020. Reservoir construction has reduced organic carbon deposition in the East China Sea by half since 2006. Geophys. Res. Lett. 47 (17), e2020GL087357.
Wang, L., Yuan, X., Xie, Z., Wu, P., Li, Y., 2016. Increasing flash droughts over China during the recent global warming hiatus. Sci. Rep. 6 (1), 30571.
Yao, P., Yu, Z., Bianchi, T.S., Guo, Z., Zhao, M., Knappy, C.S., Keely, B.J., Zhao, B., Zhang, T., Pan, H., 2015. A multiproxy analysis of sedimentary organic carbon in the Changjiang Estuary and adjacent shelf. J. Geophys. Res. Biogeo. 120 (7), 1407–1429.
Yu, M., Eglinton, T.I., Hou, P., Haghipour, N., Zhang, H., Wang, Z., Zhao, M., 2024. Apparent aging and rejuvenation of terrestrial organic carbon along the river-estuary-coastal ocean continuum. Geophys. Res. Lett. 51 (8), e2023GL107855.
Zhang, Y., Su, Y., Li, Z., Guo, S., Lu, L., Zhang, B., Qin, Y., 2022. Terrigenous organic carbon drives methane dynamics in cascade reservoirs in the upper Yangtze China. Water Res. 219, 118546.